Distribution of Solids in a Fluidized Bed Operated without a Gas Distributor

Cornelius Agu* Britt M.E. Moldestad

Department of Process, Energy and Environmental Technology
University College of Southeast Norway, 3918 Porsgrunn, Norway, {Cornelius.e.agu, britt.moldestad}@usn.no

Abstract

Despite several advantages of a gas distributor, there are also some challenges in its application. Using a gas distributor increases the fluidizing gas compression cost. Due to deposition of fine particles and product of chemical corrosion, the gas flow area across a distributor may also be reduced. This paper investigates the distribution of solids in a fluidized bed operated without a gas distributor. The gas supply is through two opposite points on the column wall. In this bed configuration, the fluidized bed behaviour simulated using the CPFD (Computational Particle-Fluid dynamics) Barracuda code is compared with an equivalent system where a uniform gas distribution is assumed. For different powders with mean size 480 – 710 μm, the results show that the axial distribution of pressure fluctuation in both types of bed configurations are similar, particularly near the bottom of the bed. The relative solid fraction fluctuation is lower than 0.2 around the central axis and it spans over 21 – 83% and 41 – 65% of the bed diameter, respectively. These results therefore show that stable bubbling behaviour and good distribution of solids can also be achieved in a bed operated without any distributor.

Keywords: Gas distributor, CPFD Barracuda, Fluidized bed, Pressure fluctuation, Solids fraction

1 Introduction

A gas distributor is usually used in fluidized bed operations. There are different types of gas distributors including porous plates, perforated plates and tuyere nozzles (Paiva et al., 2004; Kunii and Levenspiel, 1991). A gas distributor helps to ensure uniform gas distribution to achieve a stable operation. However, due to pressure drop across the distributor, gas-pumping cost through a fluidized bed can be high in operation. In chemical reactors, the gas passage (pores for porous plate or holes for perforated plate) can be clogged by fine particles, products of corrosion or sintered particles.

In addition, gas distributor design influences the performance of a fluidized bed. The selection of a suitable distributor usually depends on the operation and particle size group (Kunii and Levenspiel, 1991). For a stable operation, Zuiderweg (1967) proposed that a ratio for a distributor pressure drop to the overall pressure drop can be selected from the range 0.2 – 0.4. Different literatures (Sobrino et al., 2009; Paiva et al., 2009) have investigated the effect of a distributor on a fluidized bed behaviour. Although, some studies employ larger particles at the bottom of a bed as a gas distributor, no available literature has described the performance of a bed without a gas distributor. The aim of this study is to investigate the distribution of solids in a fluidized bed operated without a gas distributor.

The behaviour of a bed without a distributor has been studied in a set of experiments conducted with three different particles with mean size in the range 480 – 710 μm. The pressure drop along the bed and axial distribution of relative pressure drop fluctuations for a system without any gas distributor are compared with those obtained from an equivalent bed fitted with a porous distributor plate. The results are briefly presented in this paper. The bed behaviour at the lower part of the bed was not investigated due to lack of experimental data. In this study, further investigation into the bed behaviour is carried out using the CPFD (Computation Particle-Fluid Dynamics) codes. This study therefore presents the simulated distribution of pressure fluctuation along a bed and distribution of solids fluctuation across the fluidized bed operated without a gas distributor. The results are compared with the simulated results for an equivalent system where a uniformly distributed gas flow is applied at entrance of the bed.

2 Materials and Methods

2.1 Experimental

Table1 shows the properties of the particles and the minimum fluidization velocities obtained from the two different bed configurations. The experiments were performed in an 8.4 cm diameter cylindrical column and height 1.4 m with pressure sensors fitted at different locations along the column axis.

As can be seen in Table 1, the minimum fluidization velocity in both cases are very close for each of the

https://doi.org/10.3384/ecp18153248

Proceedings of The 59th Conference on Simulation and Modelling (SIMS 59), 26-28 September 2018, Oslo Metropolitan University, Norway

Table 1. Bed properties for different particles with the associated range of superficial air velocity.

Material	Sieve size range (μm)	Mean particle diameter (μm)	Density (kg/m^3)	Initial bed solids fraction (-)	U_{mf} (m/s)	
					With plate	Without plate
Limestone	450 - 1100	701	2837	0.478	0.382	0.390
Sand	400 - 1000	685	2650	0.544	0.320	0.330
Sand	100 - 700	484	2650	0.545	0.172	0.180

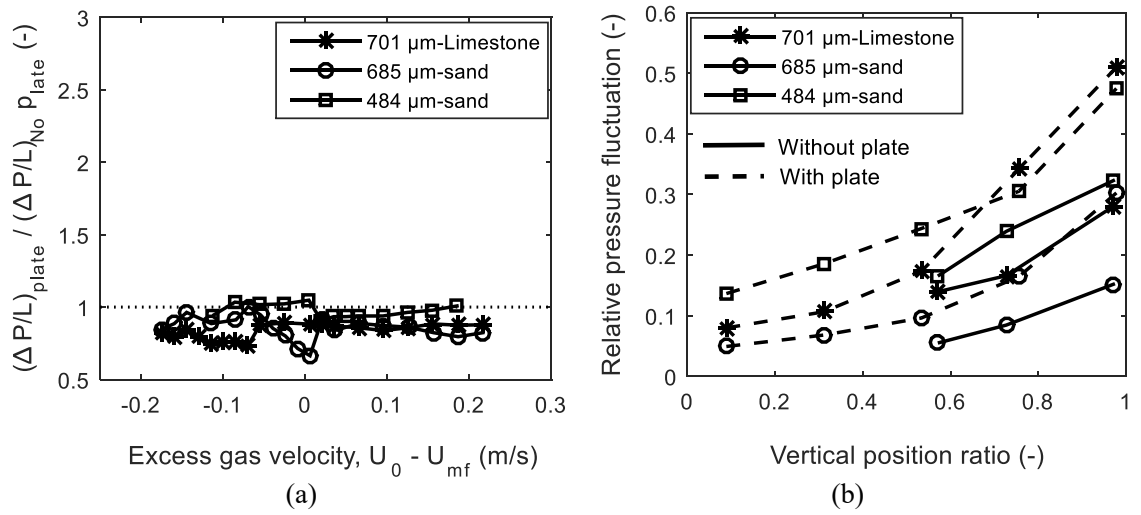

Figure 1. Experimental data (a) pressure drop ratio between a bed with porous plate and without any plate (b) axial distribution of pressure fluctuation comparing two bed cases. U_0 = 0.571, 0.481 and 0.361 m/s for the 701 μm, 685 μm and 484 μm particles, respectively.

powders. In Figure 1 (a), the experimental study shows that the pressure drop in the bed operated with a distributor is relatively lower than that without any distributor, where $(\Delta p/L)_{plate}/(\Delta p/L)_{No\ plate} < 1$. Moreover, since $(\Delta p/L)_{plate}/(\Delta p/L)_{No\ plate} < 1$ when $U_0 - U_{mf} > 0$, it shows that there is no channeling effect in the bed without a distributor. Here, $\Delta p/L$ is the pressure drop per unit length measured across the bed height, U_0 is the superficial gas velocity and U_{mf} is the minimum fluidization velocity of the bed. For the same particle sizes in Table 1, the axial distribution of the pressure drop fluctuations measured above the middle of the bed also shows that a bed operated without a gas distributor is more or less stable than that with the distributor plate within the same section of the bed; see Figure 1(b).

However, the performance of a bed without the gas distributor is believed to have been influenced by the particle size and bed diameter. In the experimental setup, two 4 mm gas entry points are installed at two opposite sides near the bottom of the bed. With these gas introduction points in such a smaller diameter bed, uniform gas distribution may be achieved before the gas flows up to the middle of the bed.

2.2 Computational

The CPFD model is based on the two distinct phases between the fluid and the solids particles. The fluid phase is modelled based on the Eurerian continuum approach while the particles motion is based on the Lagrangian particle tracing approach. For the fluid phase, the mass balance is expressed as

$$\frac{\partial(\varepsilon_g \rho_g)}{\partial t} + \nabla.\left(\varepsilon_g \rho_g \boldsymbol{u}\right) = 0 \quad (1)$$

Here, $\boldsymbol{u}(u_x, u_y, u_z)$ is the gas velocity, where u_x, u_y and u_z are the respective velocity components in the x, y and z directions and $\varepsilon_g$is the volume fractions of the gas at any section of the bed. For any given volume within the bed, the model imposes the following relationship between the two phases.

$$\varepsilon_g + \varepsilon_s = 1 \quad (2)$$

where, ε_s is the volume fraction of the solid phase. The momentum balance in the gas phase is described by

$$\frac{\partial(\varepsilon_g \rho_g \boldsymbol{u})}{\partial t} + \nabla\left(\varepsilon_g \rho_g \boldsymbol{u}.\boldsymbol{u}\right) = -\nabla p_g - \boldsymbol{f_d} + \varepsilon_g \rho_g \boldsymbol{g} + \nabla.\varepsilon_g \boldsymbol{\tau_g} \quad (3)$$

Here, $\boldsymbol{\tau_g}$ is the gas shear tensor and $\boldsymbol{g}(0,0,-g)$ is the acceleration due to gravity. The momentum exchange rate per unit volume $\boldsymbol{f_d}$ between the fluid and the individual particle can be obtained from

$$\boldsymbol{f_d} = \iint fm\left(\beta(\boldsymbol{u} - \boldsymbol{v}) - \frac{1}{\rho_s}\nabla p_g\right) dmdv. \quad (4)$$

For the solids phase, the momentum balance is based on the Lagrangian approach such that particles of similar

Table 2. Simulation parameters for the CPFD models.

Parameters	Description	With plate	Without plate
$\boldsymbol{T}$ (K)	Operating temperature	300	300
$\boldsymbol{\rho}$ (kg/m^3)	Air density	1.2	1.2
	Inlet air flow	Mass flow rate	Mass flow rate
$\boldsymbol{h_0}$ (m)	Initial bed height	0.450	0.485
$\boldsymbol{\varepsilon_{s0}}$ (-)	Initial solids volume fraction	Fixed bed solids fraction; see Table 1	Fixed bed solids fraction; see Table 1
$\boldsymbol{d_p}$	Particle size	Sieve size range; see Table 1	Sieve size range; see Table 1
$\boldsymbol{\varepsilon_{s,max}}$ (-)	Close pack solids volume fraction	0.64	0.64
Grid	Rectangular		
$\boldsymbol{\Delta t}$ (s)	Time step	0.001	0.001
$\boldsymbol{t_{sim}}$ (s)	Total simulation time	30	30

properties are grouped together and the group is treated as one particle. The grouping of particles is made on the basis of their sizes, densities and shapes. The individual particle in each group is assumed to be located at position $\boldsymbol{x_s}(x_s, y_s, z_s)$, where x_s, y_s and z_s are the position coordinate of the particle. The motion of the particles is described as in Eqs (5) and (6).

$$\frac{d\boldsymbol{v}}{dt} + \nabla\left(\varepsilon_g \rho_g \boldsymbol{u}.\boldsymbol{u}\right) = \beta(\boldsymbol{u} - \boldsymbol{v}) - \frac{1}{\rho_s}\nabla p_g + \boldsymbol{g} - \frac{1}{\varepsilon_s \rho_s}\nabla.\boldsymbol{\tau_s}, \quad (5)$$

$$\frac{d\boldsymbol{x_s}}{dt} = \boldsymbol{v} \quad (6)$$

Here, $\boldsymbol{v}(v_x, v_y, v_z)$ is the solids velocity in the bed, β is the interphase drag coefficient and $\boldsymbol{\tau_s}$ is the inter-particle normal stress. The detailed descriptions of the CPFD model and its numerical scheme can be found elsewhere (Chen et al., 2013).

In the fluid-particle system, the drag model greatly influences the accuracy of the CFD simulation results. Several drag models can be found in the literature (Wen and Yu, 1966; Gibilaro et al., 1985; Gidaspow, 1994), and a number of these are included in the drag model library of the Barracuda software.

The CPFD model is simulated using the commercial software supplied by the Barracuda AS. The simulations are based on the two different geometries shown in Figure 2 for the two cases described in section 3. In the case with a distributor plate, the fluid flow at the inlet boundary is defined at the bottom of the column. The air velocity at the downstream of the distributor is assumed uniform across the cross-section of the bed. The pressure drop across the distributor and its influence on the hydrodynamic of the bed at different air velocities are not considered in this simulation. For the case without a distributor, the inlet airflow rate is defined at the two opposite sides of the column wall as shown in Figure 2(b).

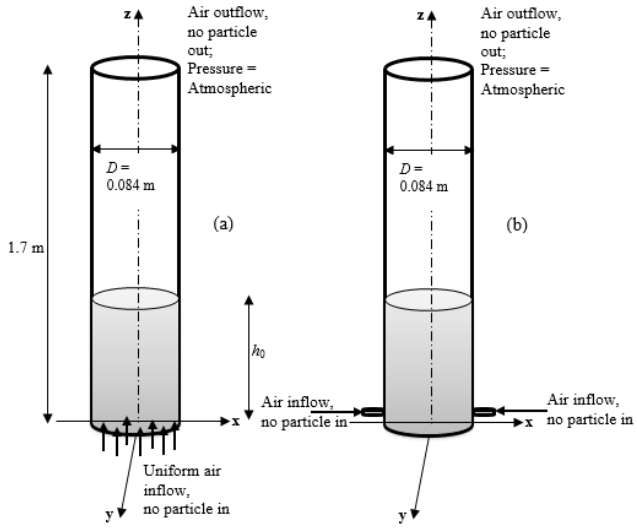

Figure 2. Computational domain for simulation of fluid-particle system with (a) uniformly distributed airflow from the bottom (b) airflow from the sidewalls.

By default, Barracuda generates uniform number of grids across a given cross-section within a computational domain. In this simulation, rectangular grids are used, and their sizes are as shown in Table 2. Also shown in the table are the parameters used in the simulations. The Wen and Yu (1966) drag model is used with the default settings as given in the Barracuda 17.05 version. In this study, the model simulations are used to qualitatively compare the solids distribution and movement between the two cases, and for this reason, all the parameters for particle-particle interactions are left at the default setting in the Barracuda software.

3 Results and discussions

Fluctuation of fluid pressure along a bed height and radial distribution of solid particles in a fluidized bed are simulated using the CPFD Barracuda code. With these simulated results, the behaviour of a bed operated

without any gas distributor is compared with its equivalent system operated with a gas distributor. These two different bed configurations are referred to as Case A and Case B, respectively in this discussion. For Case A, gas is introduced as a jet at two opposite sides of the computational domain as shown in Figure 2, and for Case B, a uniform gas flow distribution is introduced from the bottom.

Figure 3 shows the pressure drop per unit length simulated from the CPFD code for a bed of 685 µm sand particles at different gas velocities. Comparing with the experimental data, the results show that the code predicts the bed behaviour with a good accuracy. The trend of the pressure drop simulated agrees well with the overall pressure drop measured at plenum side of the experimental set up. For estimating the minimum fluidization velocity at the point of maximum pressure drop, the simulated result is compared with the pressure drop profile obtained in the middle of the bed. As can be seen, the simulated minimum fluidization velocity 0.33 m/s agrees very well with the experimental value 0.32 m/s.

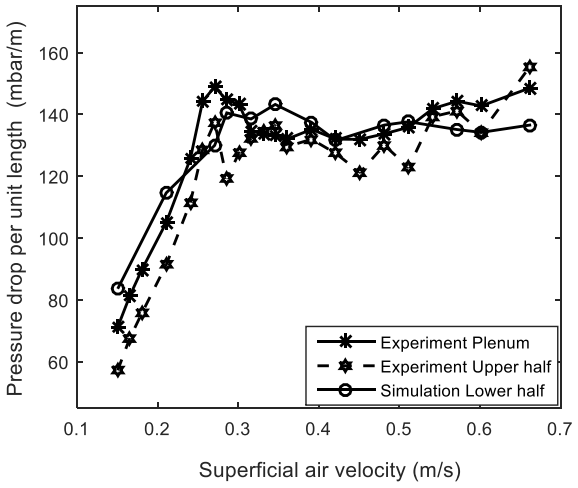

Figure 3. Variation of pressure drop with superficial air velocity in the bed of 685 µm sand particles, comparing the simulated with the experimental results at increasing gas flow rate.

3.1 Axial distribution of relative pressure fluctuation

Pressure fluctuation in a fluidized bed is mainly due to rising of bubbles in the bed (Bi, 1994). With an increase in the gas velocity, the fluctuation of pressure drop in a bed increases due to an increase in bubble size. Figure 4 shows the distribution of pressure fluctuation (computed as the standard deviation of the absolute pressure measured over a period) along the vertical axis in a bed of 685 µm sand particles. This result shows that the pressure fluctuation decreases along the bed height at a given gas velocity. The decreasing value in the pressure fluctuation is associated with a decrease in the fluid pressure up the bed height. The result also shows that the trend of the simulated pressure fluctuation using the CPFD code agrees with that of the experiment, although quantitatively, there is a significant difference. Within the dense region of the bed, both results show that the fluctuation is slightly constant but decreases rapidly above this region. This also indicates that the fluid pressure fluctuation can be associated with the movement of bulk of particles in a fluidized bed.

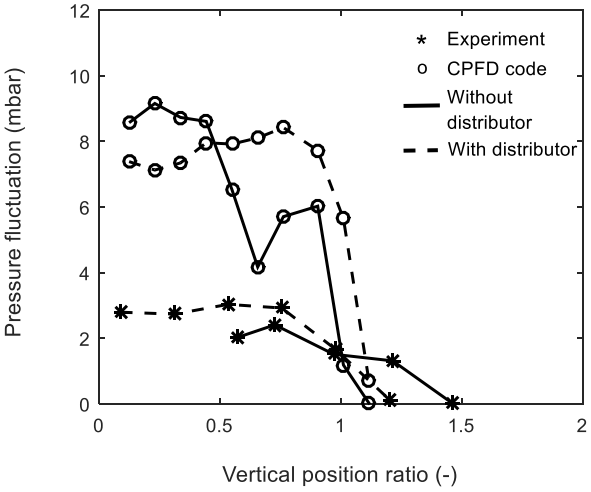

Figure 4. Distribution of absolute pressure fluctuation along the bed height for 685 µm sand particles at U_0=0.481 m/s.

However, Figure 4 shows that the absolute pressure fluctuation is more or less chaotic along the bed height due to uneven distribution of bubble activities (coalescence and splitting). With this chaotic behaviour, it will be difficult to compare the hydrodynamics of a bed in the two cases A and B. It can also be seen that the bed fluctuation associated with bubble rise is hidden. Bubbles often grow in size as they rise up a bed. Large bubbles carry significant amount of solid particles in their wakes and when they erupt near the surface of the bed, it results in a relatively higher bed fluctuation. Hence, normalizing the pressure fluctuation with the average fluid pressure will be a good tool for comparing bed behaviour in different fluidized bed systems of the same particle properties. Here, the normalized pressure fluctuation is referred to as the relative pressure fluctuation.

Figure 5 compares the relative pressure fluctuation simulated along the bed height for the two cases. As can be seen, the curve of relative pressure fluctuation increases smoothly along the bed. The relative fluctuation is higher in case B than in case A for both powders: 685 µm and 484 µm sand particles. A higher relative pressure fluctuation indicates a flow of a larger bubble volume. Comparing case A with B, the results in Figure 5 agree with the behaviour obtained in the experiment as shown in Figure 1. Closer to the surface of the bed, the fluctuations are much larger in case B (with plate) than in case A (without plate).

Moreover, similar to case B, Figure 5 shows that the pressure fluctuations in case A decrease smoothly along

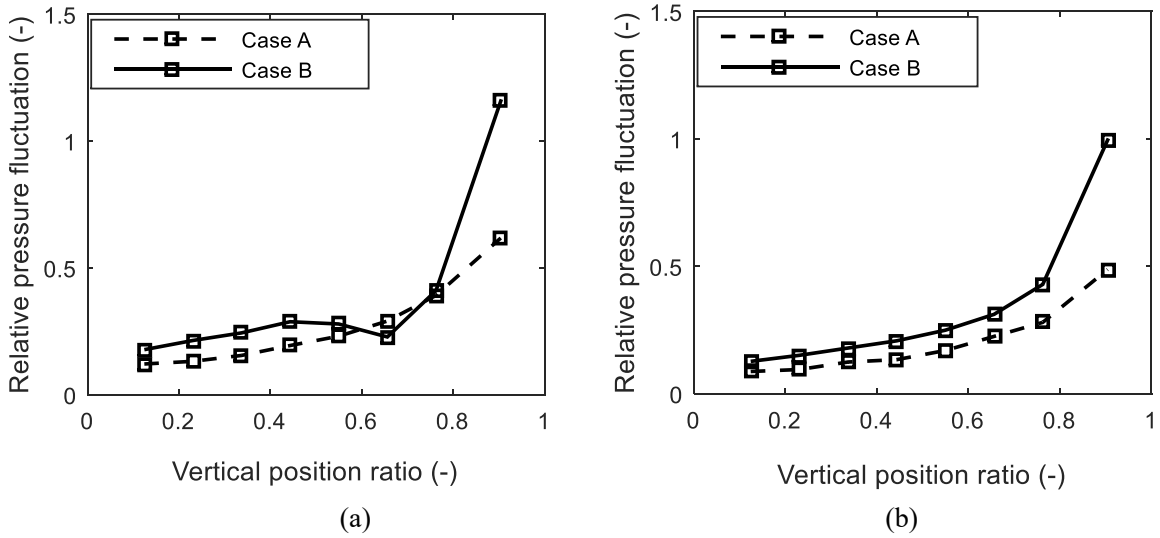

Figure 5. Distribution of relative pressure fluctuation along the bed height (a) 685 μm sand particles at $U_0 = 0.481$ m/s (b) 484 μm sand particles at $U_0 = 0.27$ m/s.

the negative bed axis, which shows that the behaviour at the lower part of the bed without a distributor is as stable as that operated with a gas distributor.

3.2 Radial distribution of solids fraction and axial velocity

Figure 6 shows the radial distribution of the relative solids fraction fluctuation obtained in the middle ($h = 22.5$ cm) of the bed for both cases A and B. The relative solid fraction fluctuation measures the degree of solid movement, and thus the solids mixing across a bed. Similar to the relative pressure fluctuation, the relative solid fraction fluctuation is obtained by diving the standard deviation by the average solid fraction at each position in the bed radial direction. The results show that the solids movement is more pronounced around the column walls in both cases. Near the central axis of the bed, the degree of solids movement is higher in case B than in case A. The solids fluctuations also vary among the different powders at the same radial position. The variation is shown to be more dependent on the gas velocity above the minimum fluidization velocity than on the particle size. As $U_0 - U_{mf}$ increases, the solids fraction fluctuation increases. In Figure 6(b), the solids fraction fluctuations for the bed of 685 μm sand particles at any radial position and the corresponding values for the 701 μm limestone particles bed are closer to one another since the value of $U_0 - U_{mf}$ is almost the same for both beds. For the case in Figure 6(a), the relative solids fraction fluctuations are almost identical, irrespective of the bed material, particle size and the excess gas velocity.

However, solids fraction fluctuations do not absolutely indicate the direction of movement of the particles. The fluctuations are brought about either by the upwards or downwards movement of the particles. Figure 7 shows the solids vertical velocities in both cases for the different particle types. The results show that the solid particles move upwards near the walls and downwards towards the centre of the bed. The speed of the solids along the central axis also increases with increasing value of $U_0 - U_{mf}$ as shown in the figures. Along the central axis, the solids speed in the bed of case B is higher than that in the bed of case A. Comparing Figures 6 and 7, it can be seen that the solids fraction fluctuations are greatly influenced by the upwards movement of the particles than by their downwards movement. Since the solids upwards movement is associated with the rise of bubbles, it shows that the solids fraction fluctuation and thus the mixing of solids, are influenced by the rising bubbles in the fluidized beds.

4 Conclusion

Including a gas distributor in a fluidized bed system can help to achieve a uniform gas distribution and stable operation. However, there are still some operational challenges in using a gas distributor. This study investigated the distribution of pressure fluctuation along a bed height and solids movement across the bed when it is operated without any gas distributor. The study was based on simulations using the CPFD Barracuda code.

For three different powders with mean size in the range 480 – 710 μm, the simulated axial pressure distribution was compared with the experimental data,

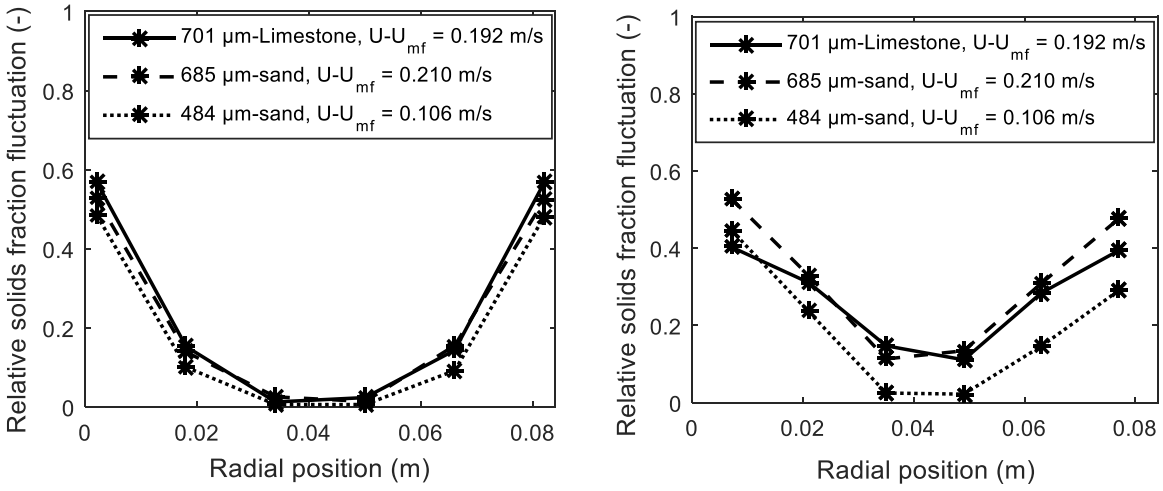

Figure 6. Radial distribution of the relative solids fraction fluctuations in the middle of the beds with (a) Case A (b) Case B.

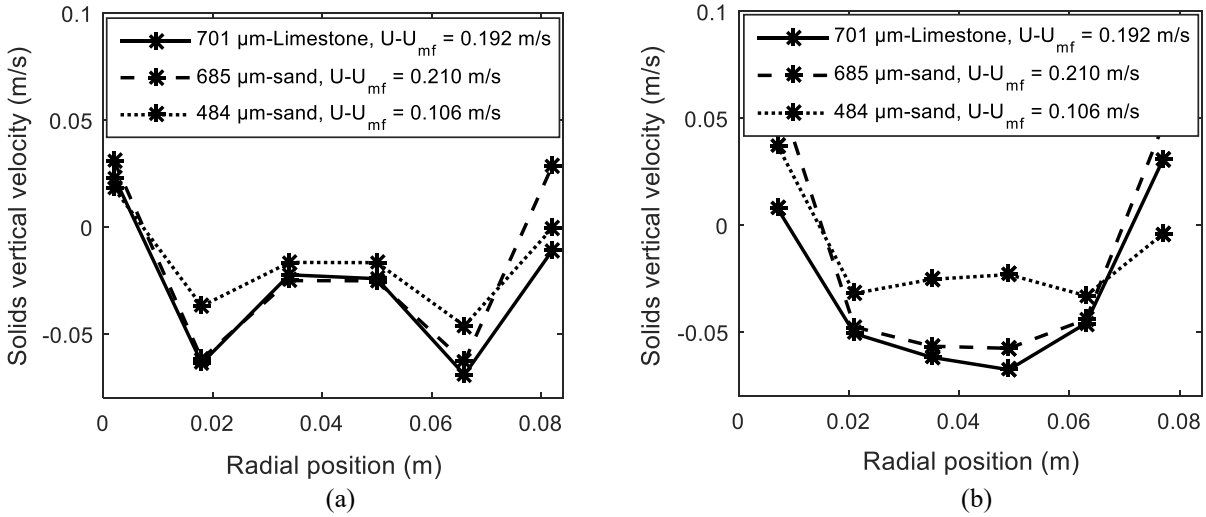

Figure 7. Radial distribution of the solids velocity in the middle of the beds with (a) Case A (b) Case B.

and the results showed that the model predicted the behaviour observed in the experimental data. The absolute pressure fluctuation is almost constant within the dense region of the bed, but decreases rapidly above this region. However, the pressure fluctuation normalized with the average pressure drop increases smoothly along the bed height, indicating an increase in the bubble size and bubble velocity along the bed. The results also show that within the lower region of the bed, the difference between the axial pressure fluctuation for a bed without a distributor and that where a uniform gas distribution is assumed is quite small, but significant at the upper region of the bed. As the relative pressure fluctuation decreases smoothly down the bottom of the bed, it also shows that the bubbling behaviour of the bed operated without a gas distributor is not affected due to absence of a distributor, particularly in the lower part of the bed. The relative solid fraction fluctuation is lower than 0.2 around the central axis and spans over 41 – 65% and 21 – 83% of the bed diameter for the cases with gas distributor and without gas distributor, respectively. This indicates that there is better mixing behaviour with a uniformly distributed gas flow in the bed.

In all, further investigations are required to ascertain the optimum number of gas entering points and their distribution for efficient operation of a fluidized bed without a gas distributor.

References

Paiva J.M., Pinho C. and Figueiredo R. The influence of the distributor plate on the bottom zone of a fluidized bed approaching the transition from bubbling to turbulent fluidization. Chemical Engineering Research and Design, 82: 25 - 33, 2004.

Kunii D. and Levenspiel O. Fluidization Engineering, 2nd ed., Butterworth – Heinemann, Washington Street, USA, 1991.

Zuiderweg F.J. Design Report on Fluidization. In Proceedings of International Symposium on Fluidization, A.A.H. Drinkenburg, ed., P. 739, Netherlands University Press, Amsterdam, 1967.

Sobrino C., Ellis N. and Vega M.D. Distributor effects near the bottom region of turbulent fluidized beds. Powder Technology, 189: 25 – 33, 2009.

Paiva J.M., Pinho C. and Figueiredo R. Influence of the distributor plate and operating conditions on the fluidization quality of a fluidized bed. Chemical Engineering Communications, 196: 342 – 361, 2009.

Chen C., Werther J., Heinrich S., Qi H-Y. and Hartge E-U. CPFD simulation of circulating fluidized bed risers. Powder Technology, 235: 238 – 247, 2013.

Wen C.Y. and Yu Y.H. Mechanics of fluidization. Chemical Engineering Progress. Symposium, 62: 100 – 110, 1966.

Gibilaro L.G., Felice R. Di and Waldram S.P. Generalized Friction Factor and Drag Coefficient for Fluid-Particle Interaction. Chemical Engineering Science, 40: 1817 – 1823, 1985.

Gidaspow D. Multiphase Flow and Fluidization: Continuum and Kinetics Theory Descriptions, Academic Press Inc., San Diego, California, USA, 1994.

Bi X. Flow Regime Transitions in Gas-Solid Fluidization and Transport, PhD Thesis, Department of Chemical Engineering, the University of British Columbia, 1994.